J Nanostruct 9(2): 331-339, Spring 2019

RESEARCH PAPER

Fabricant and characterization of $SrWO_4$ and novel silver-doped $SrWO_4$ using co-precipitation method: Their photocatalytic performances for methyl orange degradation

Farideh Sedighi[1], Ali Sobhani-Nasab[2,3], Mahdiyeh Esmaeili-Zare[1], Mohsen Behpour[1,]*

[1] *Institute of Nano Science and Nano Technology, University of Kashan, Kashan, Iran*

[2] *Social Determinants of Health (SDH) Research Center, Kashan University of Medical Sciences, Kashan, Iran*

[3] *Core Research Lab, Kashan University of Medical Sciences, Kashan, Iran*

ARTICLE INFO

Article History:
Received 21 October 2018
Accepted 17 September 2018
Published 01 April 2019

Keywords:
Ag°-$SrWO_4$
Co-precipitation
Photocatalysis
$SrWO_4$
Surfactant Concentration

ABSTRACT

A simple co-presipitation method has been developed to synthesize $SrWO_4$ and Ag°-$SrWO_4$ micro/nanostructures with different morphologies, including platelet-, star- and flower-like, in the presence of $Na(B(C_6H_5))$ as surfactant. The formation of platelet-, star- and flower-like shapes of particulate system was examined by electron microscopy technique. The products were characterized by X-ray diffraction, scanning electron microscope, UV-vis absorption, energy dispersive X-ray and fourier transform infrared spectra. The scheelite type tetragonal structure of all the synthesized compounds was revealed by powder X-ray diffraction analysis. The influence of surfactant concentration (sodium tetraphenylborate as new surfactant) on the size and morphology of products was investigated. Finally, a good photocatalytic activity was first discovered of the Ag°-$SrWO_4$ microcrystals for the degradation of methyl orange dye after 100 min under UV-vis light. Hence, from the present investigation it was observed that the doping of Ag in $SrWO_4$ will yield a new kind of multifunctional material for fabricating electronic devices.

How to cite this article
Sedighi F, Sobhani-Nasab A, Esmaeili-Zare M, Behpour M. Fabricant and characterization of $SrWO_4$ and novel silver-doped $SrWO_4$ using co-precipitation method: Their photocatalytic performances for methyl orange degradation . J Nanostruct, 2019; 9(2): 331-339. DOI: 10.22052/JNS.2019.02.015

INTRODUCTION

Alkaline earth metal tungstants with a formula of AWO_4 (A = Ca, Sr, Ba), as a member of Scheelite-type metal tungstates, have attracted extensive interests because of their potential applications in various fields, such as optoelectronic industry, solid-state laser system, scintillator, photocatalysis, light emitting diodes (LEDs), and energy storage materials [1-8]. Strontium tungstate ($SrWO_4$), among various AWO_4 materials, belonging to a body-centered tetragonal system with WO_4^{2-} molecular ions loosely bond to Sr^{2+} cations, has attracted a great deal of attention in recent years because of their excellent physical properties [9]. In the structure of WO_4, a WO_4^{2-} anion with short W–O bond lengths consists of a central highly charged W ion without d electrons surrounded by four oxygen ions in a tetrahedral arrangement.

Over the years, many different routes were developed to obtain the $SrWO_4$ nanostructures, for example: co-precipitation [10], electrochemical [11, 12], biomimetic system of a supported liquid membrane [13], sonochemical [14], hydrothermal process [15], solvothermal-mediated micro emulsion method [16], microwave-hydrothermal [17] and cyclic-microwave [16]. The low electrical conductivity, and high recombination rate of photogenerated electron-hole pair in $SrWO_4$ nanostructures impede their practical applications [18]. In order to resolve these problems can

* *Corresponding Author Email: m.behpour@kashanu.ac.ir*

be used from deposition method of metallic nanoparticles (such as silver nanoparticle). In particular, Ag doped samples explicitly used for photocatalytic applications. The Ag nanoparticles have the unique physical and chemical properties, which are different from those of the bulk metal [19-21]. Their properties are attributed to intra-band quantum excitations of the conduction electrons [22-24], mimicking the interactions of light on metal surface via the photoelectric absorption and compton scattering.

Researchers have prepared graphene and metal ion-based hybrids, such as graphene-$SrWO_4$, Yb-$SrWO_4$, Ag°-$CdMoO_4$, Eu^{3+}-$SrWO_4$ and Ag°-$NiTiO_3$ [6,15,22,31,24]. However, there is no record found for the Ag-doped $SrWO_4$ synthesized by co-presipitation method and evaluation of its photocatalytic activity for the degradation of organic pollutants under UV light, as far as our best knowledge. Herein, we will report a facile co-precipitation method for the synthesis of Ag°-$SrWO_4$ nanocomposite as photocatalyst material to achieve improved photocatalytic activity. Besides, the effect of Sr^{2+}/surfactant ratio on the morphology and particle size of $SrWO_4$ nanostructures and Ag°-$SrWO_4$ nanocomposite was investigated. Furthermore, the as-synthesized $SrWO_4$ and Ag°-$SrWO_4$ was used as an efficient photocatalyst for the photocatalytic degradation of methyl orange (MO) dye within 100 min.

MATERIALS AND METHODS

Synthesis of $SrWO_4$ nanostructures

The $SrWO_4$ nanostructures were synthesized by a new simplistic co-precipitation method. In a typical synthesis procedure, 1 mmol of Na_2WO_4 was dissolved in the Na($B(C_6H_5)$) (as surfactants)/H_2O (hot water, typically 70 °C) mixture with the different ratios 1:0.5, 1:0.75, 1:1, 1:1.25 and 1:1.5. Afterwards, 1 mmol of $Sr(NO_3)_2.3H_2O$ was dissolved slowly into 50 ml hot solution (50 °C) under magnetic stirring. Then, the resultant solution was heated at 70 °C for 15 min under magnetic stirring, and the obtained precipitation was dried at 70 °C for 1 h. Table 1 shows the samples preparation conditions.

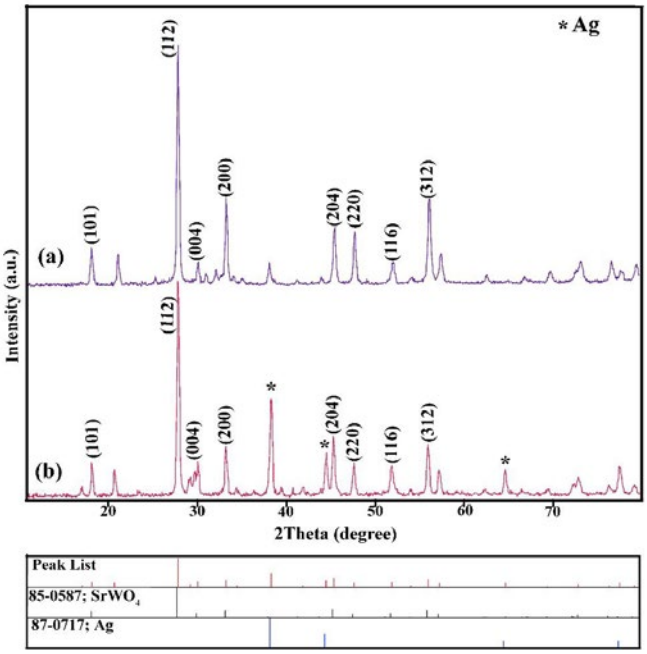

Fig. 1. XRD patterns of: (a) $SrWO_4$ nanostructure (sample No. 5), and (b) Ag°-$SrWO_4$ nanocomposite.

Table 1. Reaction conditions for preparation of products.

Sample No.	Sr/Surfactant ratio	Doping agent	Product
1	1:0.5	-	$SrWO_4$
2	1:0.75	-	$SrWO_4$
3	1:1	-	$SrWO_4$
4	1:1.25	-	$SrWO_4$
5	1:1.5	-	$SrWO_4$
6	1:1.5	Ag	Ag°-$SrWO_4$

Synthesis of Ag°-$SrWO_4$ nanocomposite

The Ag°-$SrWO_4$ nanocomposite was prepared as follows: at first, the as-prepared $SrWO_4$ nanopareticles from last past step were dissolved in the mixture of 50 ml of water and 1.8 g sodium tetraphenylborate (Sr^{2+}/ $Na(B(C_6H_5))$ ratio = 1:1.5) and then, the reaction mixture was stirred for 10 min to become homogenous. Subsequently, $AgNO_3$ solution was added to the above mixture under magnetic stirrer for 20 min at 70 °C. Then, the obtained gray powder was annealed at 500 °C for 1 h. At the end, the Ag°-$SrWO_4$ nanocomposite was obtained.

Photocatalytic experimental

The Photocatalytic activities of the $SrWO_4$ nanostructure and Ag°-$SrWO_4$ nanocomposite dissolved in water were measured by the decomposition of organic dye methyl orange (MO) under UV light illumination. In this case, 25 mg (5 ppm) of catalyst powder was added to 25 ml of dye aqueous solution at room temperature and then magnetically stirred in dark for 20 min before the irradiation to get absorption–desorption equilibrium between the photocatalyst and dye. The dye degradation percentage was calculated as:

$$\text{Degradation rate (\%)} = \left((A_0 - A_t)/A_0\right)\times 100$$

where A and A_0 are the obtained absorbance value of the dye solution at t and 0 min by a UV–vis spectrometer, respectively.

Materials and characterization

Sodium tetraphenylborate ($Na(B(C_6H_5))$, strontium

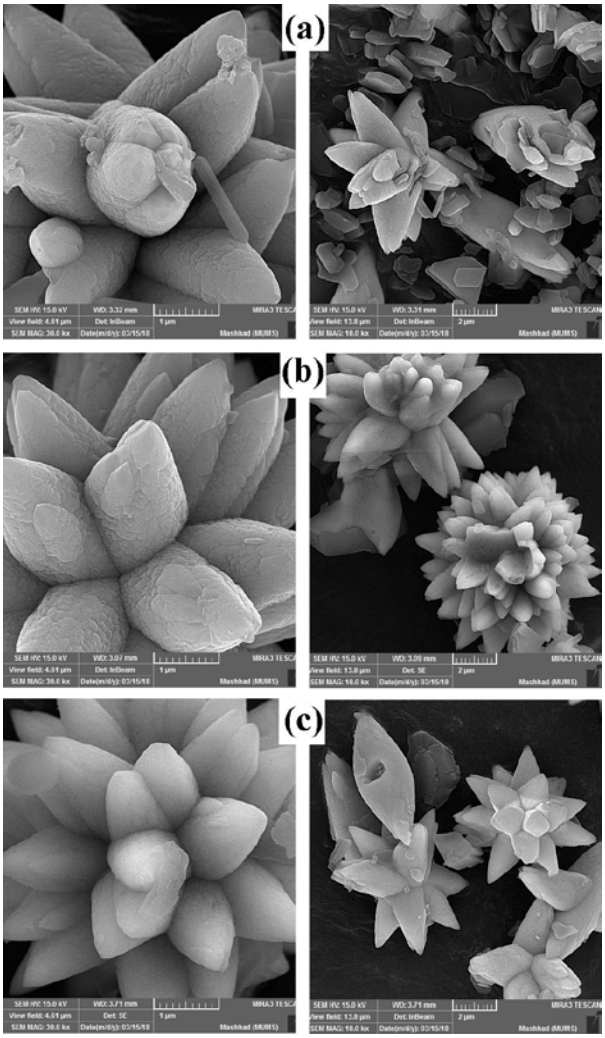

Fig. 2. (a-c) SEM images of flower-like $SrWO_4$ microcrystals (samples No. 1-3, respectively).

nitrate trihydrate and silver nitrate were applied without additional purification. The XRD patterns of the products were recorded by a Rigaku D-max C III, X-ray diffractometer using Ni-filtered Cu K_α radiation. Scanning electron microscopy (SEM) images were obtained on Philips XL-30ESEM equipped with an energy dispersive X-ray (EDX). Fourier transform infrared (FT-IR) spectra were recorded on Shimadzu Varian 4300 spectrophotometer in KBr pellets.

RESULTS AND DISCUSSIONS

The XRD patterns of samples No. 5 and 6 synthesized by co-precipitation method were shown in Fig. 1. In this figure, the diffraction peaks with the (101), (112), (004), (200), (204), (220), (116) and (312) crystal plane of scheelite type tetragonal structure $SrWO_4$ [JCPDS code 85-0587] show the as-synthesized pure $SrWO_4$ nanostructures. The XRD pattern of Ag°-$SrWO_4$ nanocomposite is similar with pure $SrWO_4$ except for absorption intensity and precise position. In Fig. 1b, the diffraction peaks at 2θ = 38.017°, 45.342° and 65.649° are related to the Ag doped in the $SrWO_4$ structure. In the XRD patterns of samples No. 5 and 6, only the tetragonal $SrWO_4$ phase were observed, that confirms the incorporation of the dopant Ag^+ ion into the $SrWO_4$ matrix.

A large volume of research has been performed to evaluate the effects of surfactants and capping agents on the morphology and particles size of nanomaterials [25–30]. Figs. 2(a-c) and 3(a and b) show the SEM images of $SrWO_4$ samples synthesized in aqueous solution using different Sr/surfactant ratios (1:0.5, 1:0.75, 1:1, 1:1.25 and 1:1.5, respectively). As shown in these figures, with the increasing of the surfactant concentration and decreasing of reaction speed between ions, the Sr^{2+} ions react with the WO^{4-} ions regularly, and product the $SrWO_4$ nanostructures with small particle size. At first, when the surfactant concentration is low, the products connected together as flower-like microcrystal structures (Fig. 2a-c), then with the increasing of Sr/surfactant ratio to 1:1.5 (Fig. 3b), the amount of flower-like structures decreased and the platelet-like $SrWO_4$ structures are produced. These structures have high surface/volume ratio, thus show better photocatalytic activity. Also, Fig. 3b displays a star-like $SrWO_4$ microcrystal formed by two rice-like $SrWO_4$ microcrystals. Fig. 4 shows a schematic representation of the synthesis and growth process of $SrWO_4$ microcrystals synthesized by co-precipitation method in the presence of $Na(B(C_6H_5))$ as surfactant. The mineralization

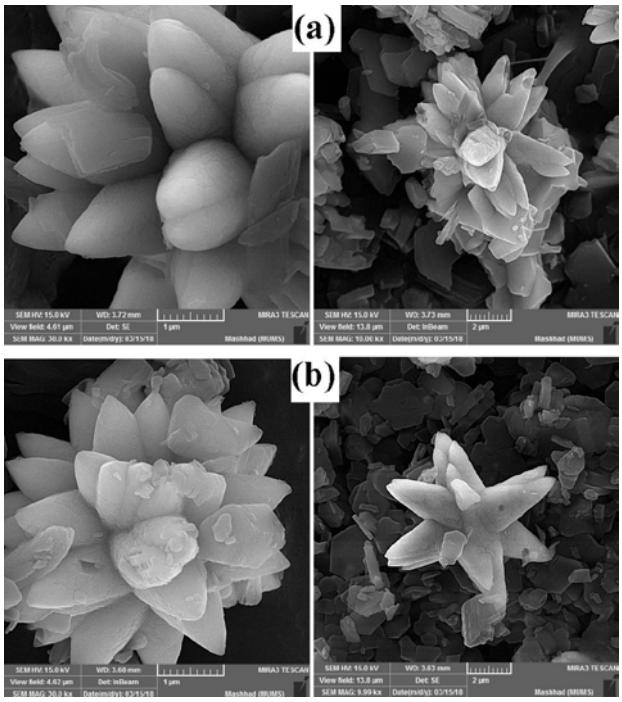

Fig. 3. SEM images of as-synthesized $SrWO_4$: (a) flower-like microcrystal (samples No. 4) and, (b) platelet- and star- like crystals (sample No.5).

process of $SrWO_4$ crystallites in aqueous solution can be divided into two steps: the initial nucleating step and the subsequent crystal growth process. In the subsequent stage, the crystal growth step is mainly a kinetically controlled process that finally can create small-size plate crystals with an evolution process.

Fig. 5 shows SEM image of Ag°-$SrWO_4$ nanocomposite synthesized using Sr/surfactant ratio of 1:1.5. As shown in this figure, with doping of silver nanoparticles into $SrWO_4$ structures, the Ag nanoparticles on the surface of rice- and star-like $SrWO_4$ crystals were formed. These nanoparticles increase the surface area of as-synthesized structures and, as a result, the photocatalytic activity is increased.

The FTIR spectra, in order to determine the chemical structure of the $SrWO_4$ nanostructure and Ag doped $SrWO_4$ in 400-4000 cm^{-1} range are given in Fig. 6(a and b). The characteristic band at 825 cm^{-1} is due to the stretching mode of O–W–O in the WO_4 tetrahedra, whereas the weak band around 489 cm^{-1} is characterized by the W–O stretching vibration [31, 32]. The bands centered at 3461 cm^{-1} and 1642 cm^{-1} can be ascribed to O–H band stretching vibration and O–H bending vibration resulting from crystal water, respectively. Compared with pure $SrWO_4$, the adsorption peak of WO_4^{2-} in Ag°-$SrWO_4$ recedes, and the positions of some spectral peaks of Ag°-$SrWO_4$ show slight shift, indicating the chemical interaction between Ag and $SrWO_4$. The stretching and flexion mode of the Sr–O and Ag is below the 150 cm^{-1} and 400 cm^{-1}, respectively, which is beyond the recorded range [33].

EDS analysis, is an analytical technique used for the elemental analysis or chemical characterization of a sample, also, can be used to estimate their

Fig. 4. Schematic representation of the growth mechanism for the $SrWO_4$ crystals obtained by the co-precipitation method.

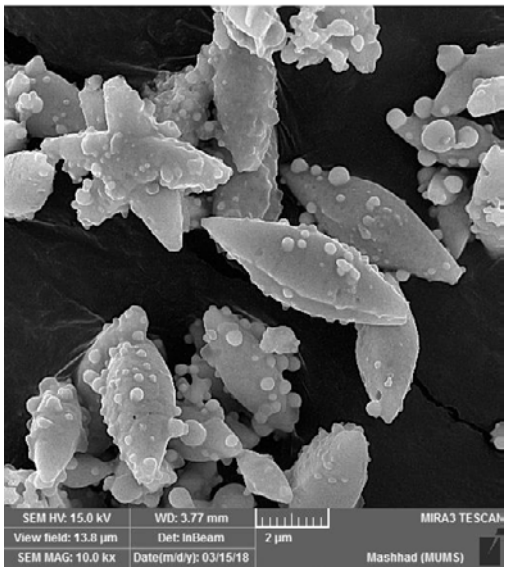

Fig. 5. SEM image of rice- and star-like $SrWO_4$ microcrystals.

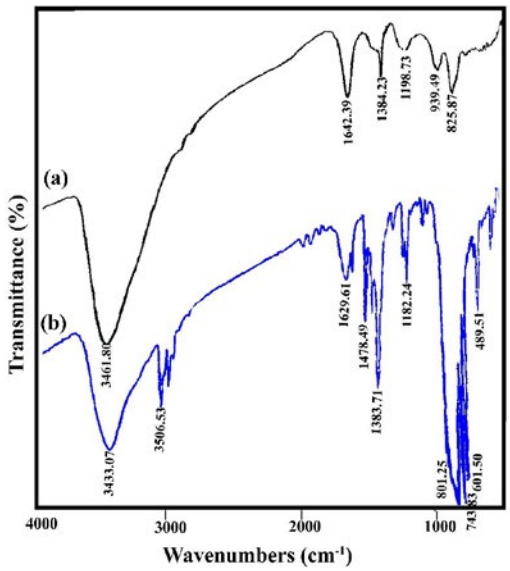

Fig. 6. FTIR spectra of: (a) sample No. 5 and (b) sample No. 6.

relative abundance. Fig. 7 shows the EDS analysis of samples No. 1-6. The EDS analysis confirms the presence of Sr, W and O elements (Fig. 7a-f) and demonstrates the availability of least amount of Ag in doped sample (Fig. 7f). Furthermore, it was also observed that the concentration of Na($B(C_6H_5)$) as surfactant influences on the atomic percentage of elements. With the increasing of Sr/Surfactant ratio to 1:1.5 (Fig. 7e), the weight percentage of Sr, W and O elements reaches to 26.12, 54.79 and 19.08%, respectively, that these values are close to stoichiometric values.

Fig. 8 displays the UV-vis diffuse reflectance spectrum (DRS) of the $SrWO_4$ samples. The DRS spectrum depicts that the product exhibited a typical optical absorption behavior of a wide-band-gap semiconducting oxide, having an intense absorption band with a steep edge [34]. The band gap of $SrWO_4$ (sample no. 5) calculated from the main absorption edge of the profile is about 4.25 eV, which is suitable for photocatalytic water splitting under UV light irradiation.

In the photocatalytic activity studies under UV excitation, MO solution was used as organic dye and its results are given in Fig. 9. The Figs. 9a and b show the photocatalyst activity of the $SrWO_4$ nanostructures and Ag°-$SrWO_4$ nanocomposite, respectively. The photocatalytic degradation of methyl orange (MO) in the presence of Ag°-$SrWO_4$ nanocomposite was very much higher compared

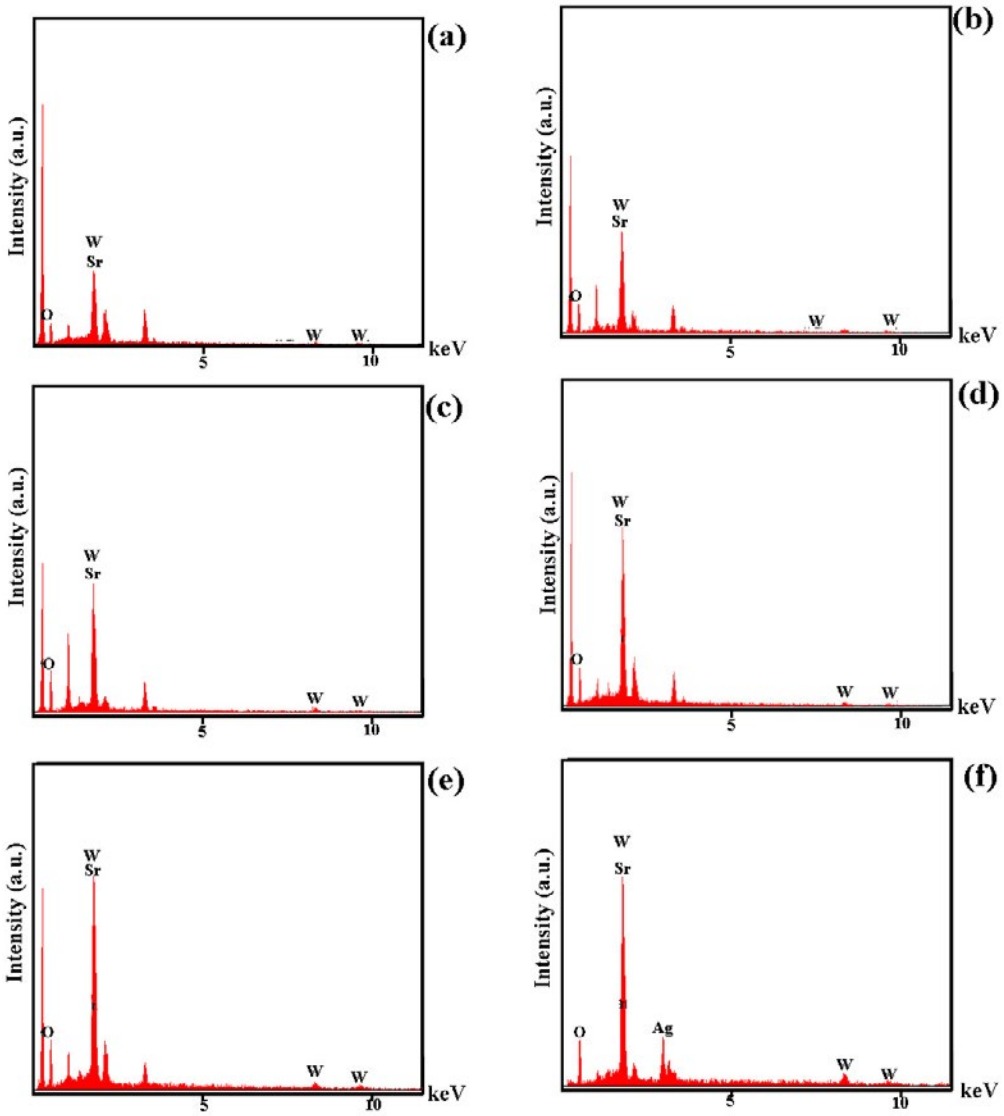

Fig. 7. (a-f) EDS spectra of samples No. 1-6, respectively.

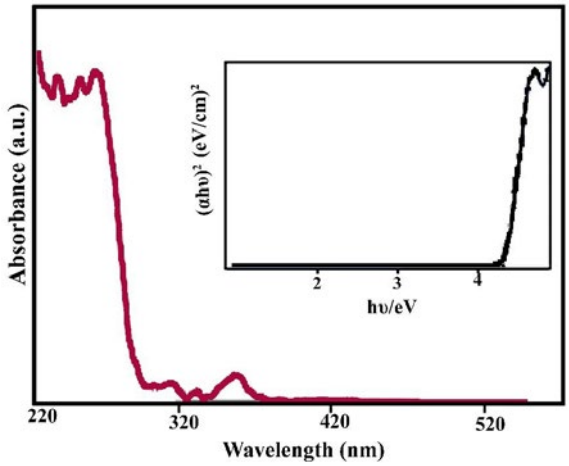

Fig. 8. UV-vis diffuse reflectance spectra of sample No. 5.

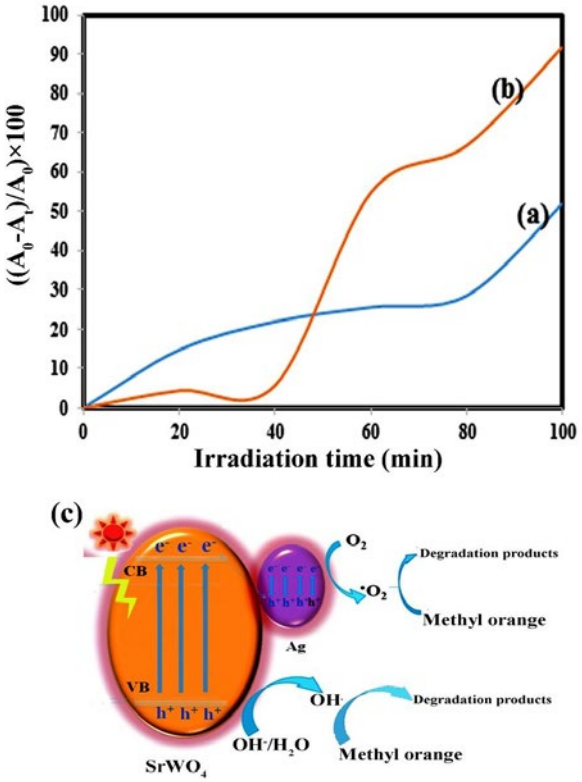

Fig. 9. (a and b) Photocatalytic activities of samples No. 5 and 6, respectively and (c) reaction mechanism of methyl orange photodegradation under UV light irradiation.

to $SrWO_4$ nanostructures [35]. It is well known that the photocatalytic activity of photocatalyst mainly results from the photo-induced electrons and holes. During UV-irradiation for 100 min, $SrWO_4$ nanostructures show 52.2% decomposition (Fig. 9a), while the Ag°-$SrWO_4$ nanocomposite shows 92.03% decomposition (Fig. 9b). Based on above experiments, a proposed mechanism for photocatalytic degradation of methyl orange by Ag°-$SrWO_4$ under UV light irradiation is shown in Fig. 8c. The valence band of $SrWO_4$ consists of the hybrid orbitals of O2p as well as Sr5s and the conduction band consists of Mo4d orbital and the band gap energies between them is

about 4.25 eV. Ag nanoparticles on the $SrWO_4$ surface, act as electron traps and enhance the electron–hole pair separation. Then the electrons on Ag° nanoparticles could be transferred to the adsorbed molecular oxygen to produce super oxide free radicals ($O_2^{-\bullet}$) and then converted to active •OH. Similarly, holes formed on the valance band of $SrWO_4$ are responsible for the oxidation of dye molecules leading to the formation of various degraded products. The degradation mechanism for the Ag°-$SrWO_4$ can be given as:

$$SrWO_4 + h\nu \rightarrow SrWO_4 (e^-) + SrWO_4 (h^+) \quad (1)$$

$$Ag^\circ + SrWO_4 (e^-) \rightarrow Ag (e^-) + SrWO_4 \quad (2)$$

$$Ag (e^-) + O_2 \rightarrow Ag^+ + O^\bullet_2{}^- \text{ (electron transfer)} \quad (3)$$

$$O^\bullet_2{}^- + H^+ \rightarrow {}^\bullet OOH \quad (4)$$

$$^\bullet OOH + H^+ + SrWO_4 (e^-) \rightarrow H_2O_2 \quad (5)$$

$$H_2O_2 + SrWO_4 (e^-) \rightarrow {}^\bullet OH + OH^- \quad (6)$$

$$SrWO_4 (h^+) + H_2O \rightarrow H^+ + {}^\bullet OH \quad (7)$$

$$SrWO_4 (h^+) + OH^- \rightarrow {}^\bullet OH \quad (8)$$

$$O^\bullet_2{}^- + MO \rightarrow \text{degraded product} + O_2 \quad (9)$$

$$^\bullet OH + MO \rightarrow \text{degraded product} + H_2O \quad (10)$$

Thus, the separation of the charge carriers was attributed to such trapping by Ag dopant in $SrWO_4$. Subsequently, enhanced the yield of •OH quantities in the degradation of methyl orange, which further improved the photocatalytic activity of Ag°-$SrWO_4$.

CONCLUSIONS

In summary, $SrWO_4$ and Ag°-$SrWO_4$ microcrystals were successfully synthesized by co-precipitation method at 70° C for the first time. We considered the effect of surfactant concentration on the size and morphology of products. The SEM images indicated that the microcrysatls, resulting in the growth of superstructures with rice, star- and flower-like shapes, were formed via self-assembly of small nanocrystals. The products were characterized by XRD, DRS, EDS, SEM and FT-IR. The Ag doped $SrWO_4$ presents enhanced photocatalytic activity compared to pure $SrWO_4$ from 52.2 to 92.03% in 100 min under UV light irradiation.

ACKNOWLEDGMENTS

Authors are grateful to the council of University of Kashan for their unending effort to provide financial support to undertake this work.

CONFLICT OF INTEREST

The authors declare that there are no conflicts of interest regarding the publication of this manuscript

REFERENCES

1. Han Y, Wang D, Liang D, Wang S, Lu G, Wang X, et al. Scheelite (CaWO4)-type microphosphors: Facile synthesis, structural characterization and photoluminescence properties. Modern Physics Letters B. 2016;30(32n33):1650400.
2. Farsi H, Barzgari Z. Chemical Synthesis of Nanostructured SrWO4 for Electrochemical Energy Storage and Conversion Applications. International Journal of Nanoscience. 2014;13(02):1450013.
3. Vidya S, Solomon S, Thomas JK. Nanocrystalline scheelite SrWO4: a low temperature co-fired ceramic optical material-synthesis and properties. Journal of Materials Science: Materials in Electronics. 2013;25(2):693-701.
4. Lou Z, Cocivera M. Cathodoluminescence of CaWO4 and SrWO4 thin films prepared by spray pyrolysis. Materials Research Bulletin. 2002;37(9):1573-82.
5. Hosseinpour-Mashkani SM, Maddahfar M, Sobhani-Nasab A. Precipitation Synthesis, Characterization, Morphological Control, and Photocatalyst Application of ZnWO4 Nanoparticles. Journal of Electronic Materials. 2016;45(7):3612-20.
6. Zhang L, Bai Q, Wang L, Zhang A, Zhang Y, Xing Y. Synthesis and electrochemical properties of SrWO4/graphene composite as anode material for lithium-ion batteries. Functional Materials Letters. 2014;07(02):1450010.
7. Sobhani-Nasab A, Sadeghi M. Preparation and characterization of calcium tungstate nanoparticles with the aid of amino acids and investigation its photocatalytic application. Journal of Materials Science: Materials in Electronics. 2016;27(8):7933-8.
8. Ahmad M, Ahmed E, Hong ZL, Xu JF, Khalid NR, Elhissi A, et al. A facile one-step approach to synthesizing ZnO/graphene composites for enhanced degradation of methylene blue under visible light. Applied Surface Science. 2013;274:273-81.
9. Liao J, Qiu B, Wen H, Chen J, You W. Hydrothermal synthesis and photoluminescence of SrWO4:Tb3+ novel green phosphor. Materials Research Bulletin. 2009;44(9):1863-6.
10. Zhao X, Cheung TLY, Zhang X, Ng DHL, Yu J. Facile Preparation of Strontium Tungstate and Tungsten Trioxide Hollow Spheres. Journal of the American Ceramic Society. 2006;0(0):060623005134010-???
11. Chen L, Gao Y. Fabrication of luminescent SrWO4 thin films by a novel electrochemical method. Materials Research Bulletin. 2007;42(10):1823-30.
12. Cui C, Bi J, Gao D. Room temperature synthesis of crystallized luminescent SrWO4 films by an adjustable galvanic cell

method. Journal of Crystal Growth. 2008;310(19):4385-9.
13. Dong F-Q, Wu Q-S, Sun D-M, Ding Y-P. Morphology-tunable synthesis of SrWO4 crystals via biomimetic supported liquid membrane (SLM) system. Journal of Materials Science. 2007;43(2):641-4.
14. Thongtem T, Phuruangrat A, Thongtem S. Characterization of MeWO4 (Me=Ba, Sr and Ca) nanocrystallines prepared by sonochemical method. Applied Surface Science. 2008;254(23):7581-5.
15. Muralidharan M, Anbarasu V, Elaya Perumal A, Sivakumar K. Band gap tailoring and enhanced ferromagnetism in Yb doped SrWo4 scheelite structured system. Journal of Materials Science: Materials in Electronics. 2015;26(9):6875-86.
16. Thongtem T, Phuruangrat A, Thongtem S. Preparation and characterization of nanocrystalline SrWO4 using cyclic microwave radiation. Current Applied Physics. 2008;8(2):189-97.
17. Sczancoski JC, Cavalcante LS, Joya MR, Espinosa JWM, Pizani PS, Varela JA, et al. Synthesis, growth process and photoluminescence properties of SrWO4 powders. Journal of Colloid and Interface Science. 2009;330(1):227-36.
18. Wang L, Wang W. In situ synthesis of CdS modified CdWO4 nanorods and their application in photocatalytic H2 evolution. CrystEngComm. 2012;14(9):3315.
19. Fu Y, Sun X, Wang X. BiVO4–graphene catalyst and its high photocatalytic performance under visible light irradiation. Materials Chemistry and Physics. 2011;131(1-2):325-30.
20. Henglein A. Small-particle research: physicochemical properties of extremely small colloidal metal and semiconductor particles. Chemical Reviews. 1989;89(8):1861-73.
21. Henglein A. Electronics of Colloidal Nanometer Particles. Berichte der Bunsengesellschaft für physikalische Chemie. 1995;99(7):903-13.
22. Mostafa Hosseinpour-Mashkani S, Maddahfar M, Sobhani-Nasab A. Novel silver-doped CdMoO4: synthesis, characterization, and its photocatalytic performance for methyl orange degradation through the sonochemical method. Journal of Materials Science: Materials in Electronics. 2015;27(1):474-80.
23. Saion E, Gharibshahi E, Naghavi K. Size-Controlled and Optical Properties of Monodispersed Silver Nanoparticles Synthesized by the Radiolytic Reduction Method. International Journal of Molecular Sciences. 2013;14(4):7880-96.
24. Mostafa Hosseinpour-Mashkani S, Maddahfar M, Sobhani-Nasab A. Novel silver-doped NiTiO3: auto-combustion synthesis, characterization and photovoltaic measurements. South African Journal of Chemistry. 2017(70).
25. Salavati-Niasari M, Soofivand F, Sobhani-Nasab A, Shakouri-Arani M, Hamadanian M, Bagheri S. Facile synthesis and characterization of CdTiO3 nanoparticles by Pechini sol–gel method. Journal of Materials Science: Materials in Electronics. 2017;28(20):14965-73.
26. Sobhani-Nasab A, Zahraei Z, Akbari M, Maddahfar M, Hosseinpour-Mashkani SM. Synthesis, characterization, and antibacterial activities of ZnLaFe 2 O 4 /NiTiO 3 nanocomposite. Journal of Molecular Structure. 2017;1139:430-5.
27. Ramezani M, Sobhani-Nasab A, Davoodi A. Bismuth selenide nanoparticles: simple synthesis, characterization, and its light harvesting applications in the presence of novel precursor. Journal of Materials Science: Materials in Electronics. 2015;26(7):5440-5.
28. Sobhani-Nasab A, Rahimi-Nasrabadi M, Naderi HR, Pourmohamadian V, Ahmadi F, Ganjali MR, et al. Sonochemical synthesis of terbium tungstate for developing high power supercapacitors with enhanced energy densities. Ultrasonics Sonochemistry. 2018;45:189-96.
29. Sobhani-Nasab A, Hosseinpour-Mashkani SM, Salavati-Niasari M, Taqriri H, Bagheri S, Saberyan K. Synthesis, characterization, and photovoltaic application of NiTiO3 nanostructures via two-step sol–gel method. Journal of Materials Science: Materials in Electronics. 2015;26(8):5735-42.
30. Sobhani-Nasab A, Rangraz-Jeddy M, Avanes A, Salavati-Niasari M. Novel sol–gel method for synthesis of PbTiO3 and its light harvesting applications. Journal of Materials Science: Materials in Electronics. 2015;26(12):9552-60.
31. Ju Z, Wei R, Gao X, Liu W, Pang C. Red phosphor SrWO4:Eu3+ for potential application in white LED. Optical Materials. 2011;33(6):909-13.
32. Eghbali-Arani M, Sobhani-Nasab A, Rahimi-Nasrabadi M, Ahmadi F, Pourmasoud S. Ultrasound-assisted synthesis of YbVO4 nanostructure and YbVO4/CuWO4 nanocomposites for enhanced photocatalytic degradation of organic dyes under visible light. Ultrasonics Sonochemistry. 2018;43:120-35.
33. Giri N, Natarajan R, Gunasekaran S, Shreemathi S. ^{13}C NMR and FTIR spectroscopic study of blend behavior of PVP and nano silver particles. Archives of Applied Science Research. 2011;3(5):624-630.
34. Sobhani-Nasab A, Hosseinpour-Mashkani SM, Salavati-Niasari M, Bagheri S. Controlled Synthesis of CoTiO3 Nanostructures Via Two-Step Sol–Gel Method in the Presence of 1,3,5-Benzenetricarboxylic Acid. Journal of Cluster Science. 2014;26(4):1305-18.
35. Pourmasoud S, Sobhani-Nasab A, Behpour M, Rahimi-Nasrabadi M, Ahmadi F. Investigation of optical properties and the photocatalytic activity of synthesized YbYO4 nanoparticles and YbVO4/NiWO4 nanocomposites by polymeric capping agents. Journal of Molecular Structure. 2018;1157:607-15.